Electronic Supplementary Material (ESI) for Journal of Materials Chemistry C.

Supplementary Information

Metal-Cyanide Hybrid Materials Exhibiting Photochromic and Photomagnetic Responses Based on Viologen Receptors

Hao Wang, [a] Teng-Da Zhou, [a] Ji-Tun Chen, [a] Han Yan, [a] Wen-Bin Sun [a]*

Table S1. Crystallographic Data and Structural Refinements Parameters for **1** and **1-P**.

	1	**1-P**
Formula	$C_{60}H_{62}Fe_2N_{18}O_{16}$	$C_{60}H_{62}Fe_2N_{18}O_{16}$
*M*r (g·mol^{-1})	1402.97	1402.97
Temperature/K	298.15	293
Space group	$P2_1/n$	$P2_1/n$
Crystal system	monoclinic	monoclinic
a (Å)	8.1707(7)	8.1584(2)
b (Å)	11.8170(10)	11.8139(3)
c (Å)	35.685(3)	35.5425(8)
α (°)	90	90
β (°)	91.123(3)	90.982(2)
γ (°)	90	90
V (Å^3)	3444.8(5)	3425.17(14)
Z	2	2
F (000)	1456.0	1456.0
Dc (gcm^{-3})	1.353	1.360
μ (mm^{-1})	0.498	4.053
R_{int}	0.0392	0.0947
limiting indice	-10 ≤ h ≤ 10 -15 ≤ k ≤ 15 -46 ≤ l ≤ 46	-9 ≤ h ≤ 7 -14 ≤ k ≤ 14 -41 ≤ l ≤ 42
Collected reflections	78744	27658
Unique reflections	7948	6044
GOF on F^2	1.057	1.101
R_1, wR_2 [I>2σ(I)]	0.0673 0.1984	0.0572 0.1562
R_1, wR_2 [all data]	0.0867 0.2157	0.0775 0.1827

[a]$R_1 = \Sigma\,||F_0| - |F_c||/\Sigma\,|F_o|$. [b]$wR_2 = \{\Sigma\,[w\,(F_0^2 - F_c^2)^2]/\Sigma\,w(F_0^2)^2\}^{1/2}$.

Table S2. Hydrogen bonds of **1**.

D	H	A	d(D-H)/Å	d(H···A)/Å	d(D···A)/Å	∠(DHA)
O4	H4	O8$^{\#1}$	0.82	1.75	2.558(4)	169.9
O5	H5	O7	0.82	1.93	2.676(6)	150.6
O8	H8C	N6$^{\#2}$	0.85	2.01	2.844(4)	168.4
O8	H8D	N2	0.85	1.96	2.812(4)	176.4
O7	H7A	N3$^{\#3}$	0.85	2.17	2.892(5)	142.1
O7	H7B	N1$^{\#4}$	0.85	1.92	2.764(4)	171.5

$^{\#1}$3/2-x, -1/2+y, 3/2-z; $^{\#2}$3/2-x, 1/2+y, 3/2-z; $^{\#3}$-1+x, 1+y, +z; $^{\#4}$+x, 1+y, +z

Table S3. Crystallographic Data and Structural Refinements Parameters for **2**.

	2
Formula	$C_{60}H_{62}Co_2N_{18}O_{16}$
*M*r (g·mol^{-1})	1403.08
Temperature/K	150
Space group	$P2_1/n$
Crystal system	monoclinic
a (Å)	8.0593(4)
b (Å)	11.7604(5)
c (Å)	35.7418(17)
α (°)	90
β (°)	91.528(2)
γ (°)	90
V (Å^3)	3386.4(3)
Z	2
F (000)	1448.0
Dc (gcm^{-3})	1.376
μ (mm^{-1})	0.568
R_{int}	0.0672
limiting indice	-9 ≤ h ≤ 9 -14 ≤ k ≤ 14 -42 ≤ l ≤ 42
Collected reflections	51654
Unique reflections	5950
GOF on F^2	1.178
R_1, wR_2 [I>2σ(I)]	0.1007 0.2458
R_1, wR_2 [all data]	0.1089 0.2522

$^a R_1 = \Sigma\,||F_0| - |F_c||/\Sigma\,|F_o|$. $^b wR_2 = \{\Sigma\,[w\,(F_0^2 - F_c^2)^2]/\Sigma\,w(F_0^2)^2\}^{1/2}$

Table S4. The curves are fitted by Orbach process for complexes **1** and **1-P** under applied dc field.

complex	dc field		τ_0 (s)	U_{eff}/κ_B (K)
complex **1**	1500 Oe dc field	Value	6.34×10^{-6}	7.84
complex **1-P**	1500 Oe dc field	Value	1.74×10^{-5}	6.22

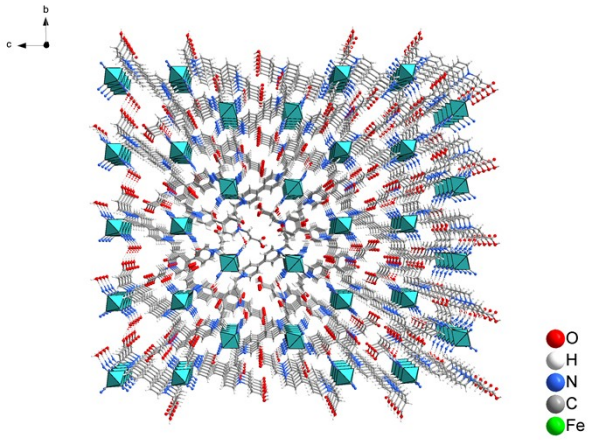

Fig. S1 The three-dimensional (3D) supramolecular hybrid structure is constructed through the linkage of ferricyanide anions and H_2Bpydp^{2+} cations via H_2O molecules.

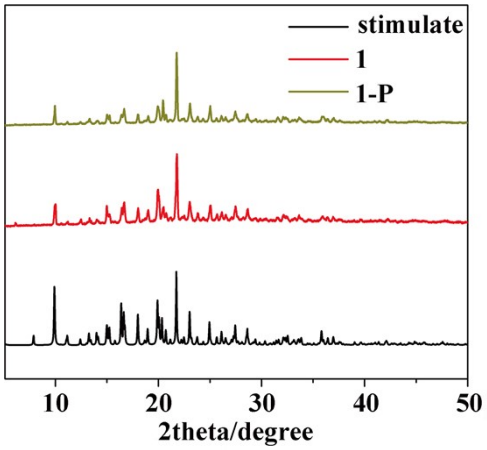

Fig. S2 The simulated and experimental powder X-ray diffraction patterns of **1** and **1-P**.

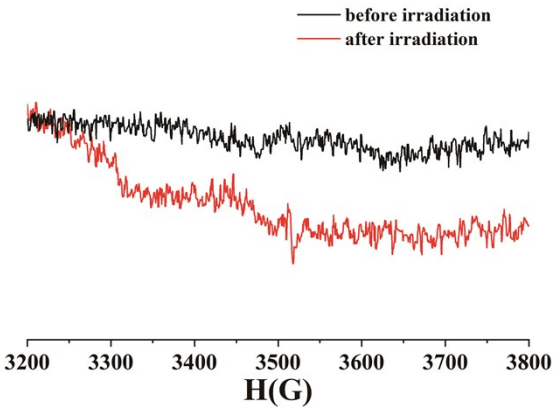

Fig. S3 ESR spectra for **1** and **1-P**.

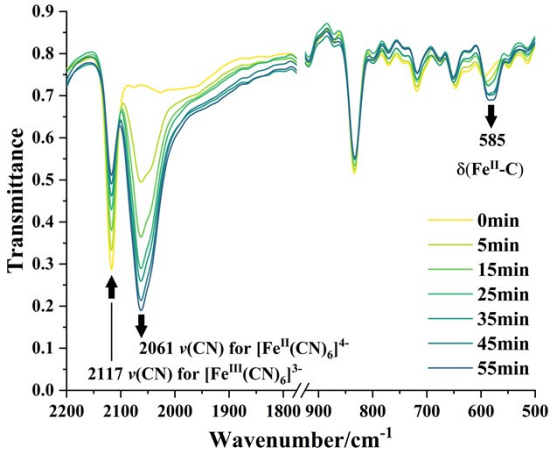

Fig. S4 Evolution of the IR spectrum of **1** in the KBr matrix upon irradiation.

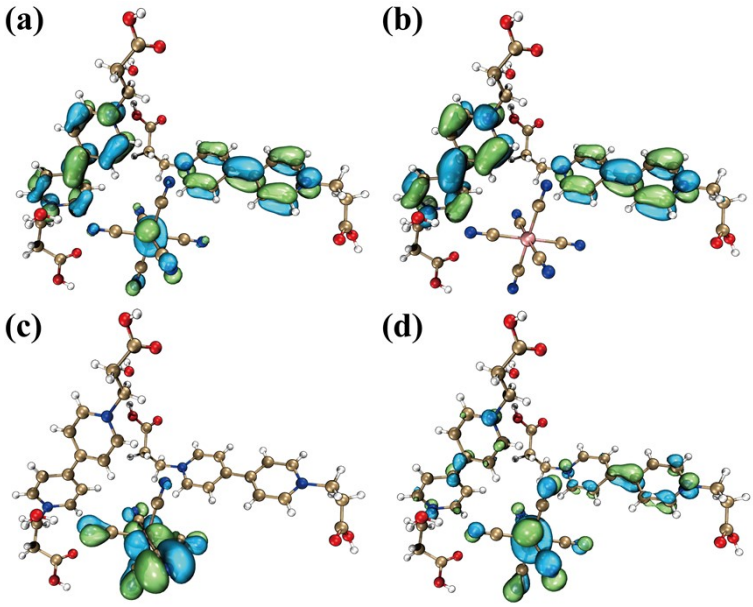

Fig. S5 HOMO (a), LUMO (b), HOMO-1 (c) and LUMO+1(d) profiles for **1**.[1, 2]

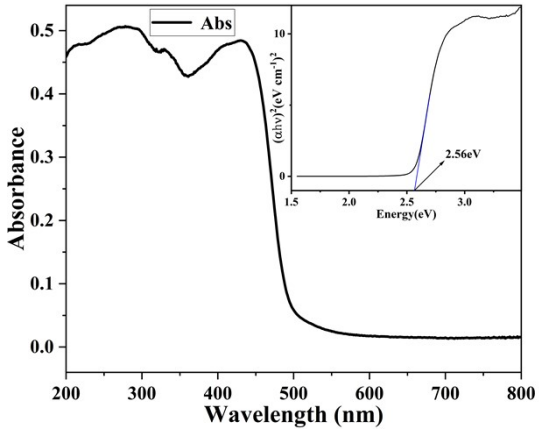

Fig. S6 The experimental band gap, determined from solid-state UV-visible spectra via the Tauc equation.

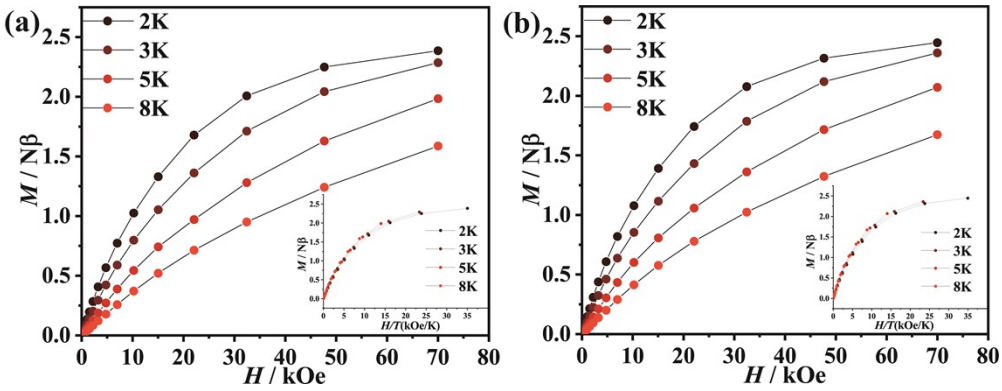

Fig. S7 Field dependence of the magnetization between 2 and 8 K for origin sample **1** (a) and colored sample **1-P** (b).

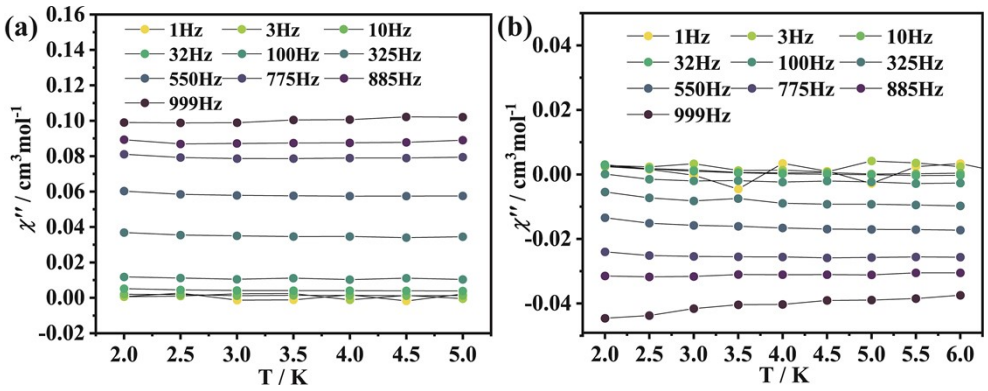

Fig. S8 Temperature-dependent curves of out-of-phase (χ'') acsusceptibility at 0 Oe for **1** (a) and **1-P** (b).

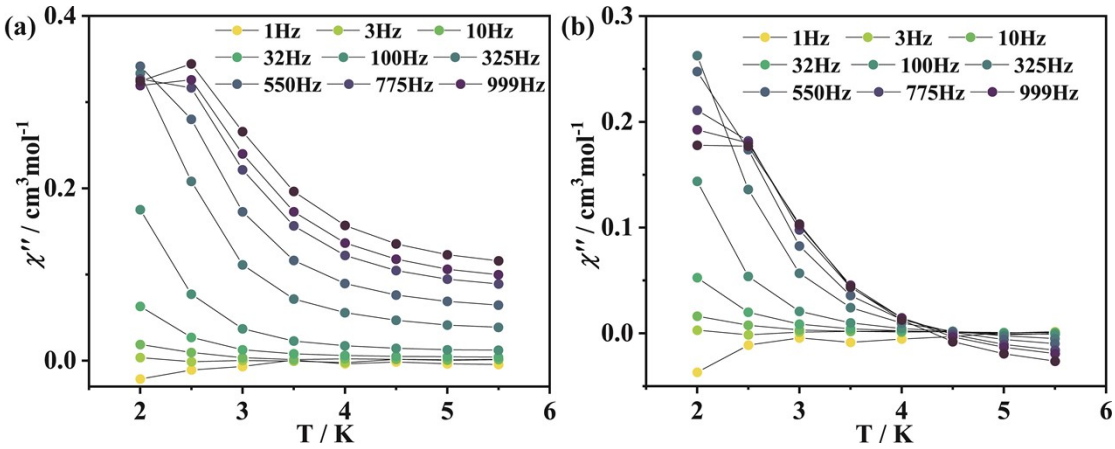

Fig. S9 Temperature-dependent curves of out-of-phase (χ'') acsusceptibility at 1500 Oe for **1** (a) and **1-P** (b).

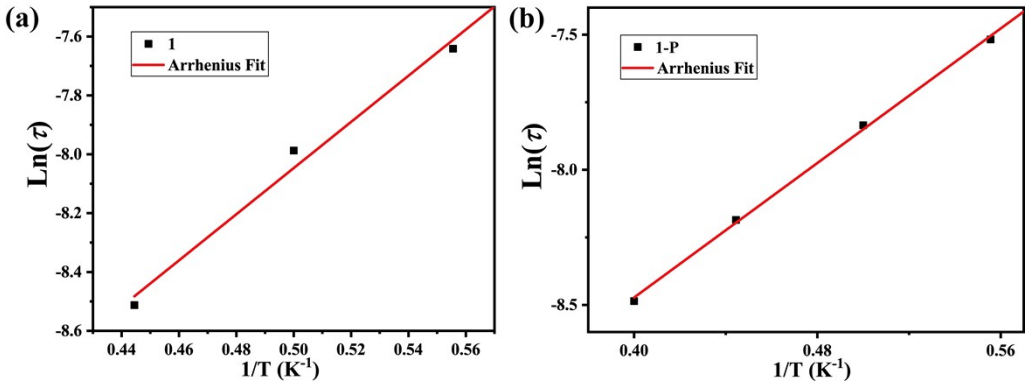

Fig. S10 Arrhenius fitting curve of the ac magnetic susceptibility of **1** (a) and **1-P** (b) under 1500 Oe.

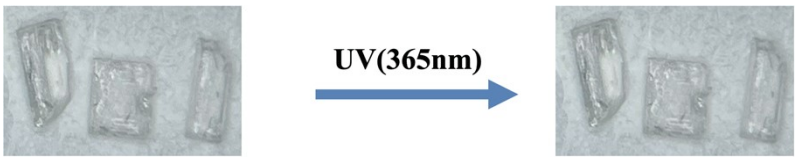

Fig. S11 The color change of **2** under UV irradiation at 365 nm.

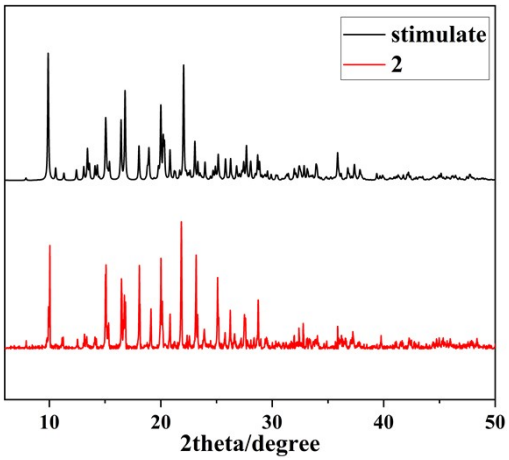

Fig. S12 The simulated and experimental powder X-ray diffraction patterns of **2**.

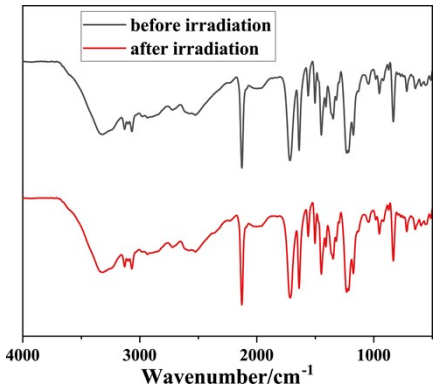

Fig. S13 The IR spectrum of **2** in the KBr matrix upon irradiation.

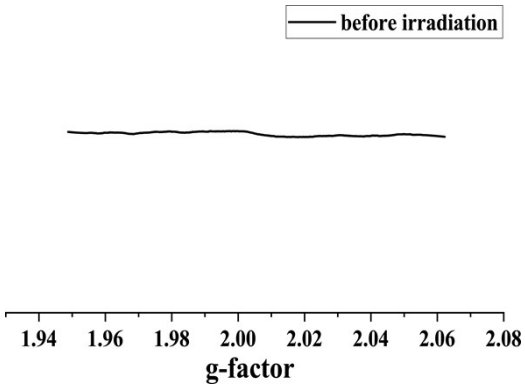

Fig. S14 ESR spectra of **2** upon irradiation.

References

[1] T. Lu, F. Chen, Multiwfn: A multifunctional wavefunction analyzer, Journal of Computational Chemistry. 33(5) (2012) 580-592. https://doi.org/10.1002/jcc.22885.

[2] W. Humphrey, A. Dalke, K. Schulten, VMD: Visual molecular dynamics, Journal of Molecular Graphics. 14(1) (1996) 33-38. https://doi.org/10.1016/0263-7855(96)00018-5.